Wireless Impedance Measurements for Monitoring Peripheral Vascular Disease

Dmitrijs Celinskis, Bruce C. Towe, Member, IEEE

Abstract—

Wireless microdevices powered by ultrasound energy have been fabricated to measure and telemeter tissue impedance spectrums for applications in peripheral vascular disease monitoring. The system is characterized by simplicity of the implant consisting of only two electrical components. *Ex vivo* testing shows the potential for constructing tissue impedance spectrum plots over the range from 10 Hz to 10 kHz by a device less than 1 mm in diameter and 1 cm long. The neurostimulator microdevice was powered by continuous waveform 650 kHz ultrasound with a swept-frequency amplitude modulation. The system was operated at safe ultrasound power levels on the order of 10-100 mW/cm^2. The device proved to be sensitive and able to measure tissue impedances over a broad range. Volume conducted signals carrying impedance information from the microdevice were remotely detected by surface biopotential electrodes.

I. Introduction

Peripheral vascular disease (PVD) results from atherosclerosis of the limb arterial circulation. It is a significant healthcare problem in the elderly population accounting for $3B/year in health care expenditures. It is accompanied by danger of limb loss and pain [1-2]. There are around 60,000 amputations resulting from PVD that are performed each year in the United States alone [3].

Tissue impedance measurements are known to reflect tissue ischemia [4], which is caused by the decrease in blood flow, and so offer a method to track the changes in PVD as a function of physician intervention. This can be useful in assessment of the treatment effectiveness, which is directed towards increase of circulation to parts of the body such as the legs. According to [4] ischemia caused by the reduced perfusion can be detected more sensitively using tissue impedance measurements than by widely used approach of pH measurements.

This work seeks to enable tissue impedance monitoring through a minimally invasive approach using a microelectronic device that can locally measure the tissue impedance spectrum and telemeter the information to the body surface. Patients with advanced PVD heal wounds slowly, thus permitting only the least invasion of tissue and excerpting the use of larger pacemaker-like devices for impedance monitoring.

The larger goal of this work is to combine impedance measurement function with peripheral limb neurostimulation performed by ultrasound powered microdevices to cause vasodilation in order to improve blood flow and for relief of pain. As part of this we develop a device to monitor the effect of interventions through impedance measurements by a device small enough potentially to be introduced through injection. Devices of small size have the advantage of avoiding silicone lead wires tunneled under the skin or through tissues.

Wireless passive yet implantable microelectronic devices of millimeter size can be realized and a number of different approaches have been proposed, involving wireless powering by magnetic induction, light, microwave energy, or ultrasound [5-9]. The smallest of these can pass through syringe needles so minimize trauma of insertion.

Biotelemetry by miniature and passive techniques have been reported [10-13], however they typically require a separate power circuit using inductive coupling and so are generally larger than that reported here.

We have previously reported the direct conversion of ultrasound energy to neurostimulation pulses [7-8]. The average electrical power requirement of neurostimulation (on the order of a milliwatt) is so low that large path losses can be tolerated since in general with this energy source much higher pulse power levels can be safely applied to the skin.

In this work we find that a variant of our previously reported ultrasound powered neurostimulator [7-8] allows, with appropriate supporting external circuitry, the measurement of the magnitude and phase of tissue impedances. This approach employs ultrasound energy to the device to provide energy to create the needed frequency swept wave that interrogates tissue impedance as well as uses volume conduction for communication to an external receiver.

II. Background

Tissue impedance measurement typically requires multiple frequency measurements to resolve both resistive and reactive components. Piezoelectric materials can convert ultrasound to electric power at efficiencies on the order of 10% under good conditions [8]. Path losses of ultrasound as it passes through tissues vary depending on the frequency and the tissue type, but a typical loss might be 1-5 db/cm

Dmitrijs Celinskis is in the School of Health and Biological Systems Engineering, Arizona State University, Tempe, AZ 85287 USA (e-mail: Dmitrijs.Celinskis@asu.edu).

Bruce C. Towe (corresponding author) is with the School of Health and Biological Systems Engineering, Arizona State University, Tempe, AZ 85287 USA (phone: 480-965-4116; e-mail: Bruce.Towe@asu.edu).

978-1-4244-7929-0/14/$26.00 ©2014 IEEE

[14-15]. Ultrasound energy at medical diagnostic frequencies in the range of 1-10 MHz is strongly attenuated by air and bone and thus, like ultrasound imaging, is limited to specific parts of the body. Lower frequencies in the range of 500 kHz-1MHz are generally more suited to powering implanted devices where bones may interfere such as the skull [15-16]. The tradeoff is that lower sound frequencies carry a lower energy density and they cannot be as well focused to the implant location. It was previously reported [7-8] that ultrasound devices can produce current flows on the order of milliamperes. In reported work on impedance measurements [4,17-18] applied current flows are in the range of 10-500 microamperes.

For purposes of blood vessel vasodilation in the lower limbs potential target for neurostimulation is sciatic nerve [2]. The human anatomy is such that it is typically less than 5 cm or so from the nearest point of the leg surface, making ultrasound powering to the implant through muscle and fat relatively straightforward.

III. Methods

Implantable neurostimulators were constructed using a microscope to assemble the electronic components and then inserted and encapsulated in 1.3 mm diameter polyimide tubing. Figure 1 shows the basic assembly of components with the diode in parallel with a piezoelectric PZT-5A ceramic.

Components of the device were interconnected with conductive silver epoxy to a rectifier and two wire-type Pt electrodes. The Schottky diode (CDC7630, Skyworks Solutions, Inc.) has a low threshold voltage and a small SC-79 package. The device was encapsulated in medical grade epoxy (353ND, Epoxy Technology). The construction of the implants of this type is discussed in greater details in [7-8].

To demonstrate the ability of the neurostimulators to perform tissue impedance measurements three experiments

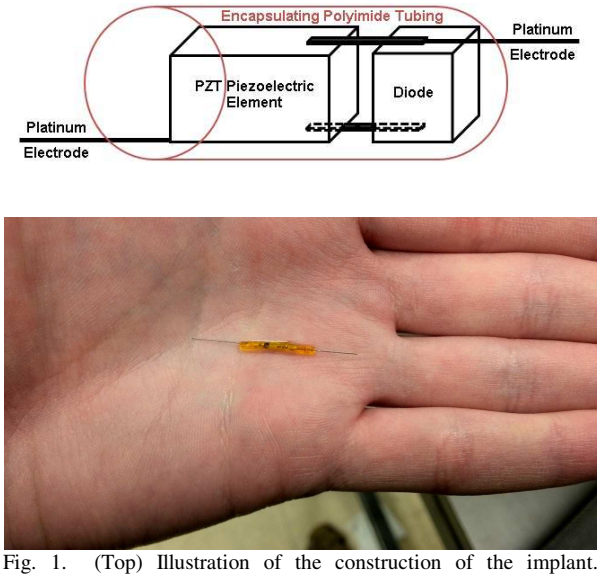

Fig. 1. (Top) Illustration of the construction of the implant. (Bottom) A photograph of the implant with platinum electrodes.

were performed, which are summarized in Figure 2.

In all cases, the setup contained a modulation signal generator (Stanford Research Systems DS345 30 MHz), carrier signal generator (Philips PM5138), amplifier (OPHIR GRF 3032), lock-in amplifier (SR530 Stanford Research Systems) and commercial focused ultrasound transducer with a center frequency of 650 kHz and diameter of 50 mm.

Carrier signal generator provides a high frequency sinusoidal signal at 650 kHz required to power ultrasound transducer, while the modulation signal generator outputs a low frequency (in the range of 10 Hz up to 10 kHz) sinusoidal signal. This low frequency signal is used to modulate high frequency carrier, which then through the amplifier is applied to the transducer. The transducer reproduces the same AM modulated signal in acoustic form, which is then applied to the implant. The PZT crystal of the device then generates an AM modulated waveform in the form of an electrical signal since it follows the external driving waveform. Next, the diode of the neurostimulator rectifies (demodulates) AM signal, causing the tissue to see the varying lower frequency modulation signal. The magnitude of the current passing through the tissue is then dependent on the tissue impedance at the modulation frequency. The skin potential from the device current flow is remotely detected by bioelectrodes and its amplitude and phase are recorded as a function of ultrasound modulation frequency.

The first experiment evaluated the device and system performance using an RC circuit which mimics tissues. In this case, neurostimulator is placed in the surface of water (with conductivity of 5 μS/cm) to provide acoustic coupling of ultrasound transducer with the implant. Electrodes of the device do not touch water and are connected to the RC

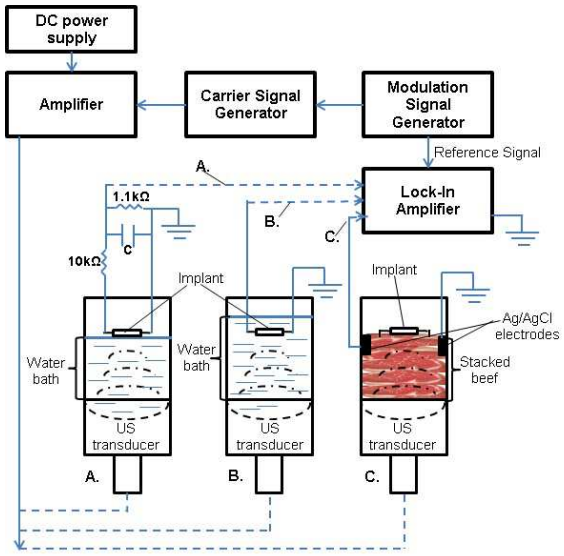

Fig. 2. Setup for *ex vivo* testing of wireless impedance measurement system. Testing involved three experiments: A. impedance measurements of an RC circuit (wired connection); B. impedance measurements of the solutions with different conductivities (wired connection); C. impedance measurements of the meat sample using surface electrodes (wireless).

circuit shown on Figure 2 (A).

The second experiment employed solutions with different conductivities. In this case an implant with electrodes is fully immersed in the solution, allowing impedance interrogation of the solution. Solutions were prepared by adding salt to the water and then introduced one after another into system shown in Figure 2 (B).

The third experiment places the implant on top of the stack of meat tissue (40 mm high) with its electrodes inserted into meat sample and implant having good contact with meat surface to ensure acoustic coupling. In this case the output of the implant is detected using Ag/AgCl surface electrodes, placed at the same height as implant's electrodes and 15 mm away from the implant's electrodes in the horizontal plane. In this experiment the impedance signal was measured remotely, without contact to the embedded device.

In all cases the RMS and phase of the signal generated by the device are measured using the lock-in amplifier, which is fed with the initial modulation signal as the reference.

IV. Results

Figure 3 presents results of the RC circuit experiment. This figure shows frequency dependent nature of the implant's output, demonstrating that implant can report impedance information consistent with that expected result from an RC model. Three curves were obtained as result of changing the capacitance value (0.47 µF, 0.22 µF and 0.1 µF) in the circuit given in Figure 2 (A). Three markers of the curves marked with red are cut-off frequencies determined experimentally for each case, but black lines – cut-off frequencies predicted theoretically.

Figure 4 was obtained employing connected wires to the device. From this figure it can be seen how magnitude and phase depend on conductivity of used solutions. This dependence is shown for four different frequencies (100 Hz, 1 kHz, 5 kHz and 10 kHz).

Figure 5 shows results of the meat tissue experiment with the impedance spectra measured wirelessly using surface electrodes. This spectrum shows that device reports changes in impedance caused by adding conductive saline solution to the meat sample.

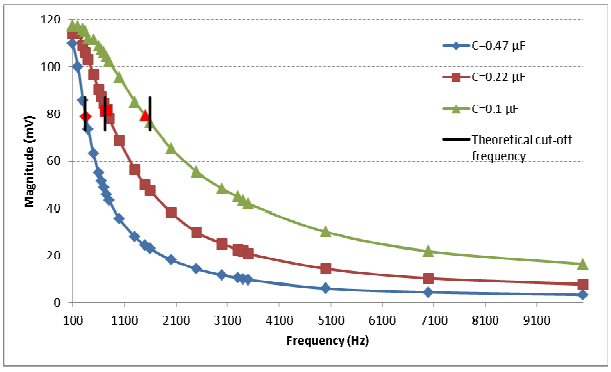

Fig. 3. Curves characterizing frequency dependence of the real part of the impedance of the RC circuit.

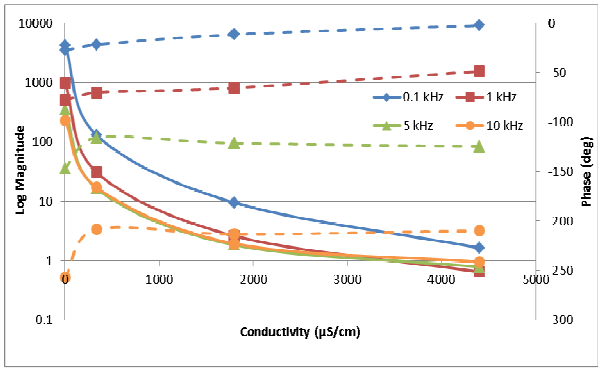

Fig. 4. Impedance magnitude and phase curves for solutions with different conductivities at four different frequencies. Magnitude (solid line), phase (dashed line).

V. Discussion

This study suggests the potential to use simple ultrasound-powered devices for tissue impedance measurements.

As it can be seen from Figure 3, the device allowed characterization of RC circuits with a cut-off frequency maximum error of 6.1%. Additionally, it can be seen that frequency dependent behavior of RC circuits corresponds to theory.

Figure 4 clearly demonstrates ability of the system to differentiate between media of different conductivities. In this case it can be done by looking to either magnitude or phase changes with changes in conductivities. As it was previously demonstrated [4,19], with increase in frequency real part of the impedance becomes less sensitive, but imaginary part becomes more sensitive to changes of the medium.

Finally, Figure 5 demonstrates fundamental ability to measure impedance wirelessly. In this case, introduction of 1 ml 335 µS/cm conductive solution into meat sample resulted in average magnitude change across all frequencies on order of 26% (in [4] impedance at zero frequency changed by about 16% due to the induced ischemia). It was also determined that at the ultrasound power levels used within present work the output of the implant can be detected using surface electrodes as far as 35 mm away from the implant (data not shown). Ultrasound power level could be increased

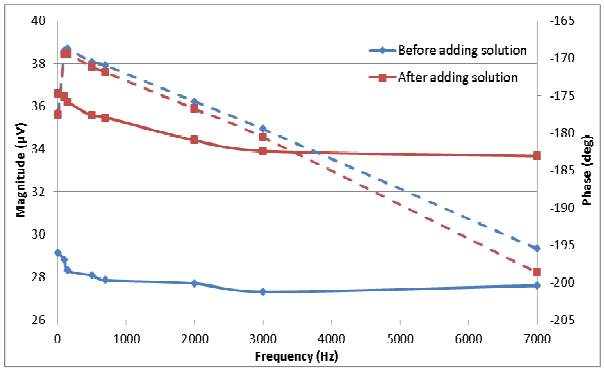

Fig. 5. Wirelessly detected magnitude and phase of the signal generated by the implant for two different impedance values (impedance change was caused by adding 1 ml of 335 µS/cm conductive solution). Magnitude (solid line), phase (dashed line).

multiple times and still be within safety guidelines.

We note that the design of the implanted device is the same as our neurostimulator previously reported [7-8,20] and thus this circuit potentially would allow a dual function. The impedance function can occur with a subthreshold drive amplitude and with the swept AM modulation and the described external circuitry.

The device is able to measure impedance changes, but not the absolute values of magnitude or phase. This however may be satisfactory since medically relevant information is often in impedance changes and in their trend with various interventions. By using algorithm described in [4] it seems to be possible to determine even absolute values, although it would require sufficient sophistication of the impedance measurement system, i.e., determination of about 13 parameters (not just phase and magnitude as in present work), swapping across 80 different frequencies, increase of the impedance spectrum recording speed, etc.

Besides PVD, potential applications of the discussed impedance measurement system can be found, for instance, in cardiology [18-19] or in brain condition monitoring [17].

VI. Conclusion

Our results demonstrate that AM modulating an ultrasound wave incident on our previously reported microstimulator then remotely detecting volume conducted currents allows real-time measurement of tissue impedance. This work demonstrates that a simple design of a potentially implantable circuit can achieve wireless tissue impedance measurement. Introduction of the impedance measurement function for the same device used to achieve neurostimulation so as to cause vasodilation leads to the possibility of a more sophisticated and more clinically useful closed loop system.

Acknowledgment

The authors would like to thank Daniel W. Gulick of Arizona State University for valuable discussions.

References

[1] Khalil, Zeinab, Merhi, Merhi, *Effects of Aging on Neurogenic Vasodilator Responses Evoked by Transcutaneous Electrical Nerve Stimulation: Relevance to Wound Healing*, Journal of Gerontology, Volume 55A, Number 6: 257-263, 2000.

[2] Park, Rae Joon et al. *The Effect of Microcurrent Electrical Stimulation on the Foot Blood Circulation and Pain of Diabetic Neuropathy*, Journal of Physical Therapy Science 23: 515-518, 2011.

[3] Huber, Stanford J., Vaglienti, Richard M., Huber, Joan S., *Spinal Cord Stimulation in Severe, Inoperable Peripheral Vascular Disease*, International Neuromodulation Society Volume 3, Number 3, 131-143, 2000.

[4] Kun, Stevan; Ristic, B.; Peura, R.A.; Dunn, R.M., "Algorithm for tissue ischemia estimation based on electrical impedance spectroscopy", *Biomedical Engineering, IEEE Transactions*, vol.50, no.12, pp. 1352-1359, 2003.

[5] A. Abdo, M. Sahin, "Feasibility of Neural Stimulation With Floating-Light-Activated Microelectrical Stimulators", IEEE Trans. Biomed. Cir. Systems, Vol. 5, no 2., p. 179 April 2011.

[6] B.C. Towe, P.J. Larson, D. Gulick, "A Microwave Powered Injectable Neurostimulator", 34th Annual International Conference of the IEEE EMBS, San Diego, Ca, USA, 28 Aug -1 Sept, 2012.

[7] P.J. Larson, B.C. Towe, "Miniature Ultrasonically Powered Wireless Nerve Cuff Stimulator", 5th International IEEE Conference on Neural Engineering 2011, pp. 265-268. : April 27 2011-May 1 2011.

[8] B. Phillips, B. C. Towe and P. J. Larson, "An ultrasonically-driven piezoelectric neural stimulator," *Engineering in Medicine and Biology Society, 2003. Proceedings of the 25th Annual International Conference of the IEEE,* 2003, pp. 1983.

[9] G. E. Loeb, R. A. Peck, W. H. Moore and K. Hood, "BION™ system for distr. neural prosthetics," *Med. Eng. Phys.,* vol. 23, pp. 9-18, 1, 2001.

[10] Neihart, N.M.; Harrison, R.R., "Micropower circuits for bidirectional wireless telemetry in neural recording applications," *Biomedical Engineering, IEEE Transactions*, vol.52, no.11, pp.1950-1959, Nov. 2005.

[11] Chestek, C.A.; Gilja, V.; Nuyujukian, P.; Kier, R.J.; Solzbacher, F.; Ryu, S.I.; Harrison, R.R.; Shenoy, K.V., "HermesC: Low-Power Wireless Neural Recording System for Freely Moving Primates", *Neural Systems and Rehabilitation Engineering, IEEE Transactions on* , vol.17, no.4, pp.330,338, Aug. 2009.

[12] Borna, A.; Najafi, K., "A low-power, low-voltage, user-programmable, wireless interface for reliable neural recording", *Biomedical Circuits and Systems Conference (BioCAS), 2011 IEEE*, vol., no., pp.77-81, 10-12 Nov. 2011.

[13] Mohseni, P.; Najafi, K., "A 1.48-mW low-phase-noise analog frequency modulator for wireless biotelemetry", *Biomedical Engineering, IEEE Transactions*, vol.52, no.5, pp.938-943, May 2005.

[14] P.N.T. *Wells. PNT, Biomedical Ultrasonics, Academic Press.*

[15] A. Denisov and E. Yeatman, "Ultrasonic vs. inductive power delivery for miniature biomedical implants," in *Body Sensor Networks (BSN), 2010 International Conference on,* pp. 84-89, 2010.

[16] S. Ozeri and D. Shmilovitz, "Ultrasonic transcutaneous energy transfer for powering implants," *Ultrasonics,* vol. 50, pp. 556-566, 5, 2010.

[17] Seoane, F.; Lindecrantz, K.; Olsson, T.; Kjellmer, I.; Flisberg, A.; Bagenholm, R., "Brain electrical impedance at various frequencies: the effect of hypoxia", *Engineering in Medicine and Biology Society, 2004. IEMBS '04. 26th Annual International Conference of the IEEE*, vol.1, no., pp.2322-2325, 1-5 Sept. 2004.

[18] Mellert, F.; Winkler, K.; Schneider, C.; Dudykevych, T.; Welz, A.; Osypka, M.; Gersing, E.; Preusse, C.J., "Detection of (Reversible) Myocardial Ischemic Injury by Means of Electrical Bioimpedance", *Biomedical Engineering, IEEE Transactions on* , vol.58, no.6, pp.1511,1518, June 2011.

[19] Schwartzman D., Chang I., Michele J.J., Mirotznik M.S., Foster K.R., "Electrical impedance properties of normal and chronically infarcted left ventricular myocardium", Journal of Interventional Cardiac Electrophysiology, 3, 231-224, 1999.

[20] B.C. Towe, T. Graber, D. Gulick, R. Herman, "Wireless microstimulators for treatment of peripheral vascular disease". In *Neural Engineering (NER), 2013 6th International IEEE/EMBS Conference on*, pages 1485–1488, Nov 2013.